Mathematical Modeling and Optimization of Pre-Acceleration BeamLine in 2MV Pelletron Accelerator

Engr. Mahnoor Farhat[1], Dr. Engr. S.M. Haider Aejaz[2]

Abstract— The 2 MV 6SDH-2 tandem pelletron accelerator installed at CASP, GC University Lahore has evolved over the past years from acceptance tests to an extremely reliable and convenient research tool in the field of particle accelerator physics, having capability of providing variety of ion beams from few keV to several MeV in energy. Many electrostatic and magnetic devices are employed to steer an ion beam in an accelerator system all the way from ion source to experimental setup. Mathematical modeling and optimization of low energy beamline has been done for this accelerator. Several ion optics and steering devices are provided in the pre-acceleration beamline for ion beam manipulation and in order to optimize the overall beam transmission. As the quality of the beam from the accelerator depends upon the design of these electrostatic and magnetic devices, optimum settings were derived by manually adjusting voltages and currents provided to low energy beamline components. From these calibrations and optimization measurements, calculations has been done for mass analysis magnets, steering and focusing components and the results has been represented. From the results, it has been found that there exists a complex relationship between the effects of different voltages and currents in order to tune the desired output current and beam profile at the end-stations. Details of experiments and data analysis are presented.

Index Terms— Pelletron accelerator, Low energy beam line, Mass analysis magnets, Einzel lens, Electrostatic steerers, SNICS II source, RF source, AccelNET control system.

1 Introduction

The pre-accelration beamline comprises of mass analysis magnet, vacuum pumps, steerers, lenses, and beam diagnostics to take the beam to a focus in the gas stripper, easily and with minimum dissipation. The Model (SW6 - 2BA017240) $\pm 30°$ inflection magnet is a double focusing model with 0.406m bend radius. It can bend the ions having mass energy product (ME/Z^2) $\leq$ 6.5 amu-MeV. To select a particular mass of ions in the ion beam, these mass analyzing magnets are employed.

To direct the mass analyzed beam to the accelerator tube, steerers and lenses are provided. The main purpose of electrostatic lenses is to focus low power energy ion beams and to fulfill specific optic requirements. The einzel lens has a specially large aperture of 63 mm diameter to reduce spherical aberrations and enhance transmission [1]. The NEC electrostatic X-Y beam steerers are used to deflect the beam in the vertical and horizontal direction by supplying high voltages to the plates. All the components are provided high voltage DC supplies for their working. The optimum values of the voltages vary according to the types and charge states of the ions as well as initially provided energies. The complex relationship between the effects of different voltages require manual hard work to tune the desired output current and beam profile.

This problem of manual tuning of current and voltages of accelerator beam handling components is solved by building a mathematical model of injection beam line. By doing this we will have different mathematical formulas expressing voltages and current of accelerator components and using these formulas we can easily find the optimum / best settings for pre-acceleration beamline so that maximum beam current will be available at the end stations.

2 Experimental Testing

2.1 Magnet current settings at pre-acceleration beamline

In this experiment, copper ions are produced using SNICS II source. By manually adjusting the source focus voltage while keeping the cathode, bias and oven voltage fixed, we obtained six data sets from AccelNET control system containing the data for switching magnet current (SM 01-1) and faraday cup current on the pre-acceleration beamline (FC 01-1). The settings for the source in our experiment is given in **Table 1.** The data sets are read in MATLAB to generate a plot between magnet current and faraday cup current. A code is written to read the text file. After the data is read, we plot both the currents, by taking the magnet current on the x-axis while faraday cup current on y-axis and find the peaks of the plot, showing the value of magnet current at which maximum faraday cup current occur. The code also calculates the masses of ions at the peak values of faraday cup current using **Eq. (1)**. The plots generated in MATLAB is shown in **Fig. 1 – 6.**

$$m = \frac{r^2 x\ q^2 x\ B^2\ x\ 1000}{(1438.5)^2\ x\ E} \tag{1}$$

Table 1 – SNICS source settings

Data sets	**Cathode voltage = 5kV, Bias voltage = 25kV, Ionizer current = 21 A, Oven voltage = 28 V, Line heater current = 19.2 A, Injection Energy = 30 keV**
	Focus voltage
1	17.16 kV
2	22.16 kV
3	12.16 kV
4	14.66 kV
5	19.66 kV
	Cathode voltage = 4 kV, Bias voltage = 10kV, Injection Energy = 15 keV
	Focus voltage
6	9.66 kV

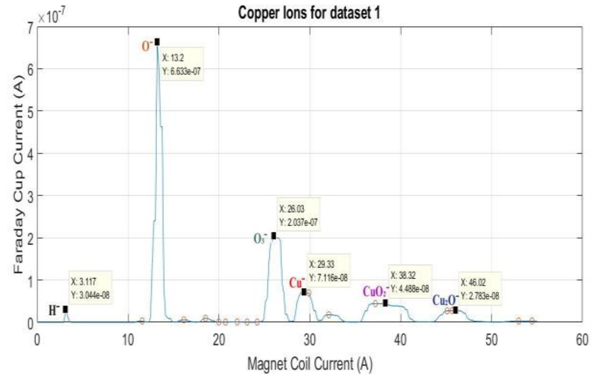

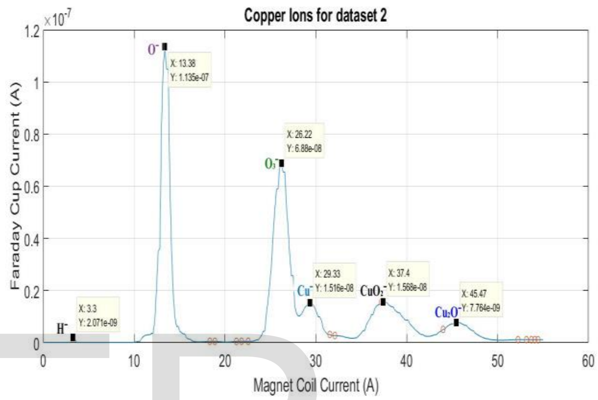

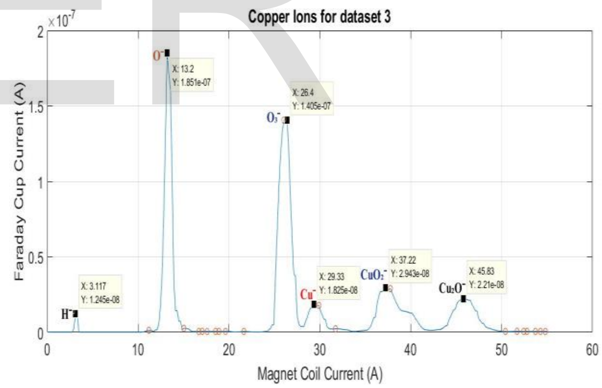

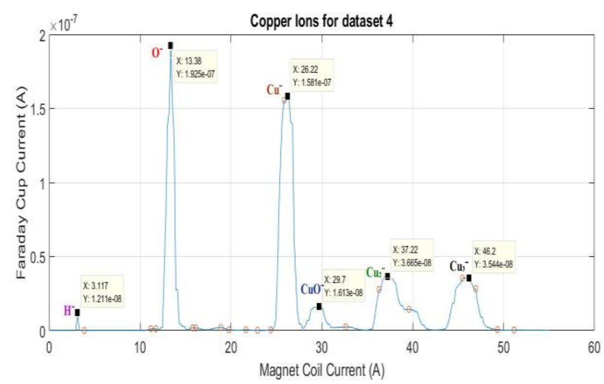

1. *Mahnoor Farhat pursued Masters degree in Electric Engineering from Government College University Lahore, Pakistan, PH- +92(331)4039906. E-mail: mahnoorfarhat6@gmail.com*

2. *Dr. Engr. S.M. Haider, PhD in Electrical Engineerng, Assistant Professor, Government College University, Lahore, Pakistan, PH-+92(333)4380572. E-mail: haideraejaz@gcu.edu.pk*

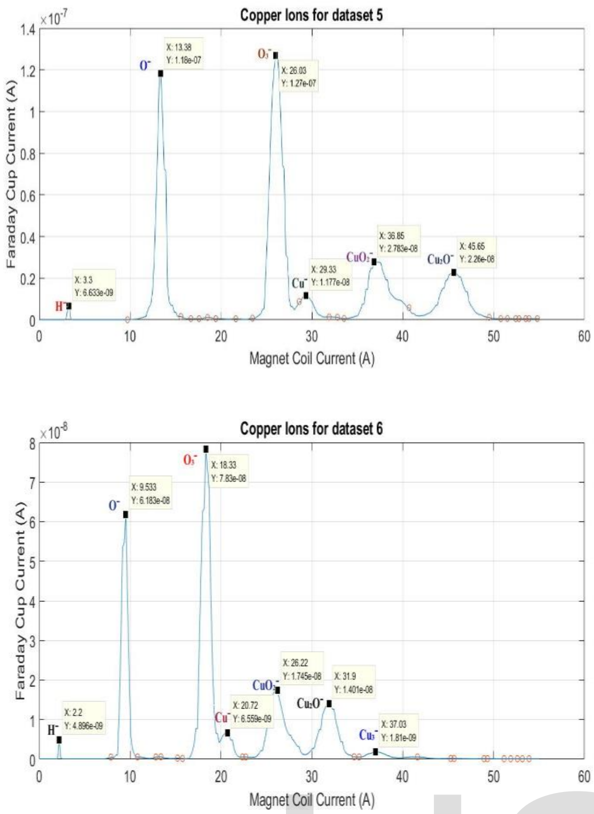

Fig. 1- 6 Magnet Coil Current vs. Faraday Cup Current for datasets (1-6)

From **Fig. 1 – 6**, it is observed that the maximum faraday cup current (FC 01-1) is obtained at 6.633 x 10^{-7} (A) for dataset 1. At this value of faraday cup current, the switching magnet current (SM 01-1) is 13.2A and the SNICS source focus is set at 17.16 kV. So the optimum settings for the magnet current is at 13.2A.

Next we observe the difference between measured value of magnet current and the calculated value by varying the atomic masses and initial energies. We obtain the formula for magnet current. By eliminating 'B' magnetic field with B = sI, s is the slope of the graph shown in **Fig. 7**. The value of slope is approximately 164.23 Gauss / Ampere**.**

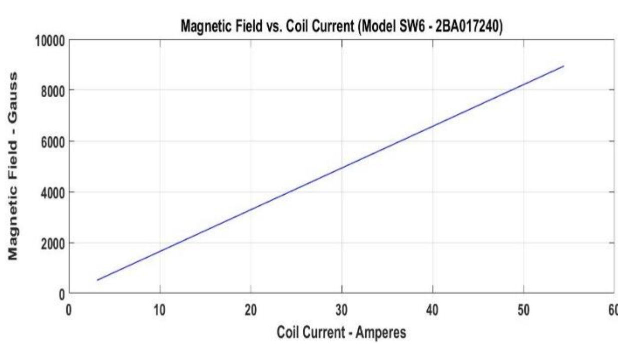

Fig. 7 Magnetic Field vs. Coil Current (Model SW6 - 2BA017240)

Table 2 shows the energies, atomic weights, optimized value of magnet current obtained from experimental work and the calculated value of this current from Eq. (2). The difference in the experimental value and calculated value for switching magnet current is represented graphically in MATLAB. **Fig. 8** shows the plot of magnet current (experimental and calculated) versus the atomic masses for H, He, Si, Cu and Au.

$$\text{Ical} = \sqrt{\frac{m \times (1438.5)^2 \times E}{s^2 \times r^2 \times q^2 \times 1000}} \quad (2)$$

Table 2 – Switching magnet current at different At. Weights and energies

Atomic weights (amu)	Hydrogen ^{1}H 1.01 amu	Helium ^{4}He 4.00 amu	Silicon ^{28}Si 28.09 amu	Copper ^{63}Cu 63.55 amu	Gold ^{197}Au 196.7 amu
INJ S1-01 (TotInjV)	30.7 kV	37.3 kV	28.7 kV	30.0 kV	31.0 kV
SM 01-1 CC	3.4 A	7.5 A	16.9 A	26.22 A	47.1 A
Calculated magnet current (A)	3.798 A	8.333 A	19.37 A	29.78 A	53.31 A

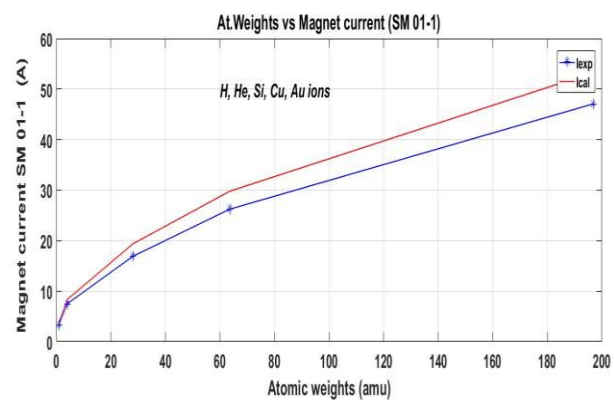

Fig. 8 At. Weights vs. Magnet current SM 01-1

A plot is also generated by keeping the atomic weight same and varying the injection energies. **Table 3** shows the varying energies, magnet current (experimental and calculated) for He and Cu ions and **Fig. 9** and **10** shows the plot between injection energies and switching magnet current SM 01-1 for He and Cu ions.

Table 3 – Switching magnet current for Cu and He ions at varying injection energies

Copper Ions		
Injection Energies (keV)	**SM 01-1 CC (A)**	**Calculated magnet current (A)**
15 keV	18.52 A	21.06 A
30 keV	19.21 A	29.78 A
Helium Ions		
Injection Energies (keV)	**SM 01-1 CC (A)**	**Calculated magnet current (A)**
32.3 keV	6.8 A	7.75 A
37.0 keV	7.3 A	8.29 A
37.3 keV	7.4 A	8.33 A
37.4 keV	7.3 A	8.34 A

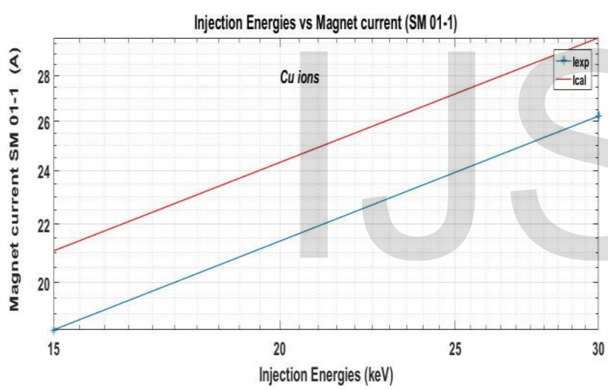

Fig. 9 Injection Energies vs. Magnet current SM 01-1 for Cu Ions

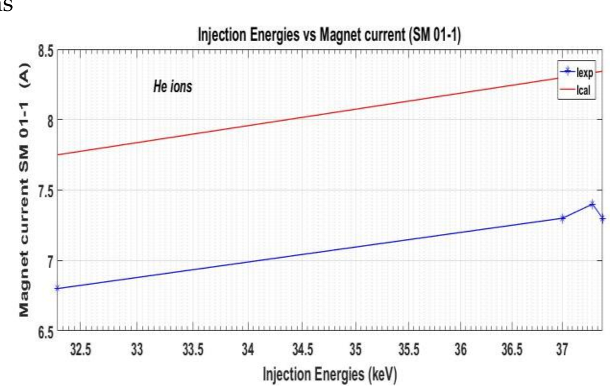

Fig. 10 Injection Energies vs. Magnet current SM 01-1 for He Ions

It is observed that the calculated value for switching magnet current on pre-acceleration beamline is approximately same with the experimental value at varying injection energies and atomic masses. As switching magnet selects a particular mass of ion, the reason for the slight difference between observed and calculated magnet current is due to contaminant beams present in the ion source. Some oxygen related beams and hydrogen beams are observed primarily from water vapor in the source. As O^- and H^- currents decrease, the required beam current will increase and this slight difference for switching magnet current (calculated and experimental value) will decrease. Hence the formula for calculated magnet current (Ical) in Eq. (2) approximately calculates the optimized value of current at different atomic weights and injector potentials.

2.2 Electrostatic steerers

Steering is required to make the beam centrally aligned. Electrostatic X-Y beam steerers as supplied with NEC Pelletrons are used to deflect the ion beams in the vertical and horizontal direction by supplying high voltages to the plates. NEC provides various versions of electrostatic steerers according to voltage ratings, length of plates and flange type. The deflection of ion beams through electrostatic steerers is independent of mass. The specifications of the model Single Axis electrostatic beam steerer available with 6SDH-2 Pelletron are given in **Table 4**. The first order deflection of a charged particle by one pair of plates is given in Eq. (3). Here,

$$\theta = \frac{Vlq}{2dE} \text{ radians} \tag{3}$$

V = potential between the plates (volts)
l = length of plates (in, cm)
q = charge on the particle (electrons)
d = separation of plates (in, cm)
E = energy of charged particle (electron volts)

Table 4 – Electrostatic Beam Steerer - Single Axis 2EA055030 specifications

Model	Single Axis 2EA055030
Plate Length	2-7/8" (7.30 cm)
Plate Separation	1.5" (3.8 cm)
Plate Width	4" (10.2 cm)
Entrance Aperture	None
Voltage rating per plate	5 kV
Material	All Metal and ceramic
Plates	Aluminum
Frame	Aluminum

The electrostatic X-Y steerers shown in **Fig. 11** are employed to reduce the angular misalignment of the beamline. Two pair of plates; x-steerers and y-steerers are used, the angular deflection is carried out by applying voltage to x-steerer plates and y-steerer plates. If the beamlines are perfectly aligned, the voltage applied to x-y steerers are zero.

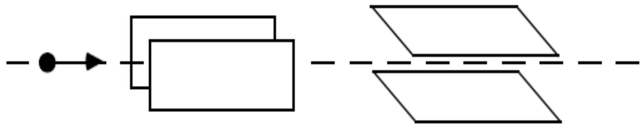

Fig. 11 Electrostatic steerer

Table 5 shows the data containing voltages applied to steerers at different injection energies, and switching magnet current (SM 01-1) for protons. It is observed that as injection energies increases, the x-steerers voltage decreases and hence the deflection angle decreases, keep in mind that deflection is independent of mass.

Table 5 – Voltages applied to the x-y electrostatic steerers for protons

Injection Energies (keV)	Switching magnet current SM 01-1 (A)	X-steerer voltage (kV)	Y-steerer voltage (kV)
30.0 keV	3.1 A	0.312 kV	0.016 kV
30.2 keV	3.1 A	0.222 kV	0.108 kV
34.4 keV	3.3 A	0.042 kV	0.106 kV
34.5 keV	3.3 A	0.036 kV	0.024 kV

Also from table, the magnet current increases as injection energy increases while keeping the mass constant. For hydrogen ions at 3.1 A of switching magnet current, the deflection required in the x-direction is more, it means the effect of switching magnet bending radius is less. While at maximum current of 3.3 A for hydrogen, the deflection required by x-steerers is less, as the beam is already aligned in the horizontal direction through switching magnets. It can be seen from Eq. (2) for magnet current. The increase in energy will result in the decrease of deflection angle and hence the applied voltage to the x-steerers. This can be represented graphically in MATLAB.

Fig. 12 and **13** shows the plot between the increasing injection energies and magnet current versus the x-steerers voltage respectively. In the case of y-steerers, where the applied voltage to the plates is zero, it means the beamline is aligned, so no deflection is required in the y-direction.

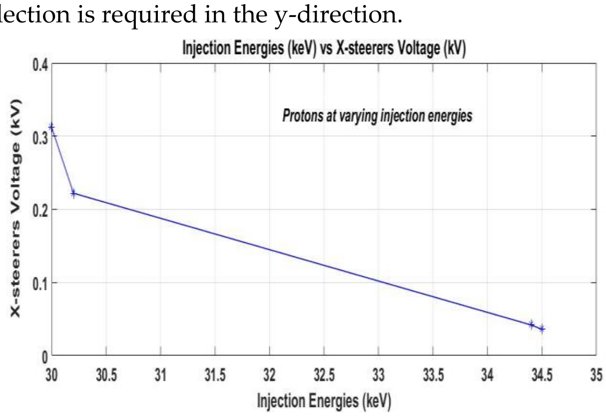

Fig. 12 Injection Energies vs. X-steerer voltage for proton

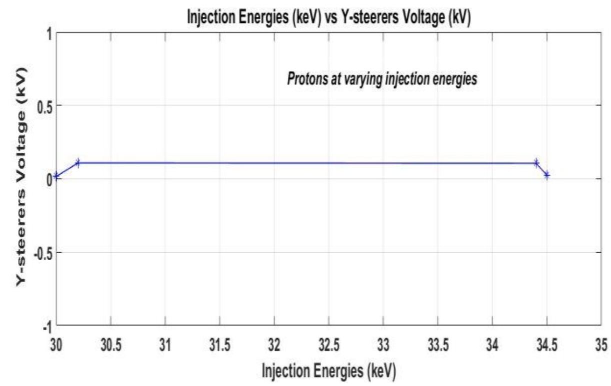

Fig. 13 Injection Energies vs. Y-steerer voltage for protons

2.3 Einzel Lens

The mass-analyzed steered beam is focused into the accelerator tank through the electrostatic lenses. The einzel lens is an electrostatic lens made by combining two gap lenses into one three-electrode system with first and last electrodes at the beam line potential V_0 and the centre electrode at a different potential V_{einzel}. After passing from the einzel lens, the energy of the ion beam remains unchanged. The einzel lens characteristics used in the low energy beam transport section is shown in **Fig. 14**.

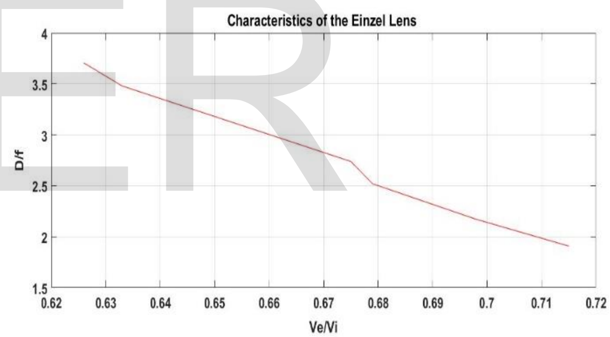

Fig. 14 Einzel lens characteristics obtained in terms of focal length normalized to aperture diameter (D/f) as a function of voltage ratio of lens

Here power of the lens (D/f) is plotted as a function of voltage ratio; the ratio between the applied to the middle electrode (Veinzel) to the voltage corresponding to the energy of injected beam (Vi). The einzel lens available with accelerator at the CASP has a specially large aperture of 63 mm diameter. The maximum voltage required for the einzel lens is 35 kV. The specifications of the model EL63-35 are given in **Table 6**.

Table 6 – Einzel lens - Model EL63-35 specifications

Model	EL63-35
Acceptance Aperture Diameter	2.50″ (63 mm)
Axial Distance Between Electrodes	0.22″ (5.6 mm)
Length Along Beamline	9″ (22.9 cm)
Electrode Voltage Rating	35 kV

Fig. 15 shows the geometry of einzel lens.

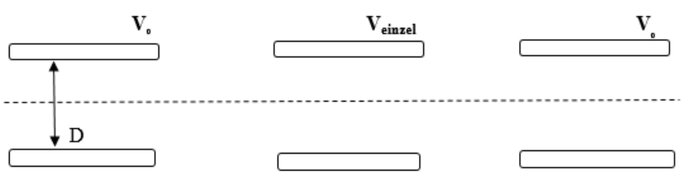

Fig. 15 Geometry of einzel lens

The focal length of an einzel lens is defined in Eq. (4) [2].

$$\frac{1}{f} = \frac{3}{8dr}(R^2 - 1)(R - 1)(3 - R) \qquad (4)$$

The focusing power of einzel lens depends on the geometry of lens and this voltage ratio. The lens has two possible configurations for R > 0, (accelerating einzel lens) and for R < 0, (decelerating einzel lens). The first gap between the electrodes of lens is accelerating and the second gap is decelerating. Both configurations are focusing. However, the refractive power of the lens is much higher in decelerating mode than in accelerating mode with the same lens voltage. We can get varying focusing conditions, by varying the einzel lens voltage V. **Fig. 16** shows the focusing 8d/3f from Eq. (4) as a function of R. **Table 7** summarizes the focusing properties of an einzel lens by varying the voltage V.

Table 7 – Einzel lenses focusing properties

V	$V < -V_1$	$-V_1 < V < 0$	$0 < V < 8V_1$	$V > 8V_1$
R	Imaginary	0 < R < 1	1 < R < 3	R > 3
1/f	No solution	> 0	> 0	< 0
	N/A	Focusing	Focusing	Defocusing

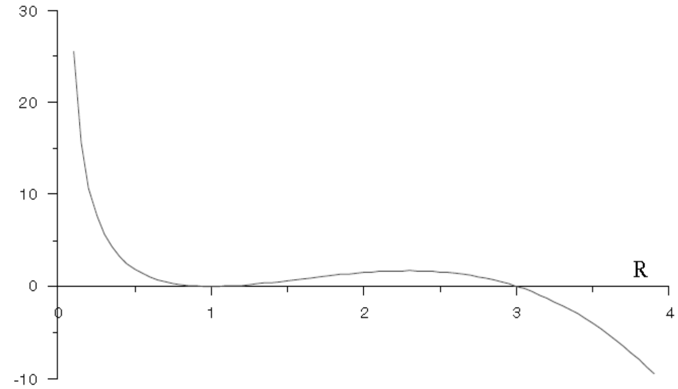

Fig. 16 Focusing 8d/3f in an einzel lens as a function of R

The einzel lens voltage ratio defines the focusing or defocusing nature of lens. Greater the ratio differs from unity, the stronger is the lens. If the ratio $V_2/V_1 = 1$, the optical power of lens is equal to zero since the equipotential regions lie at both sides of the unipotential lens, the focal lengths in the object and image spaces are equal to each other [3]. The practical focusing regime is limited to 0 < R < 1. For 1 < R < 3 the focusing is very weak and for R > 3, the Einzel lens is defocusing. **Table 8** shows data containing einzel lens voltages, respective beam currents and voltage ratios at 29.0 keV injection energy for silicon beam. We use a decelerating (negative) voltage for middle electrode of lens because it attain a stronger focus compared to an accelerating (positive) voltage [4].

Table 8 – Einzel lenses voltage ratios and focal length at 29.0 keV injection energy

Silicon ions at 29.0 keV			
Einzel lens voltage (Ve) (kV)	Voltage ratio of lens (Ve/Vb)	Ion beam current at FC 02-1 (A)	Focusing (1/f) (m)
-18.18	0.626	4.92×10^{-5}	58.82
-18.37	0.633	4.14×10^{-5}	55.24
-19.59	0.675	1.00×10^{-5}	43.47
-19.71	0.679	1.00×10^{-5}	40.00
-20.25	0.698	1.00×10^{-10}	34.48
-20.74	0.715	1.00×10^{-10}	30.30

Fig. 17 and **18** shows the plot between voltage ratio of lens versus ion beam current and focal length (1/f) respectively. It can be seen from figure that as the lens voltage (Ve) increases, the R gets closer to unity, indicating weak focusing. The trend in the beam current at faraday cup on post acceleration beamline is also shown.

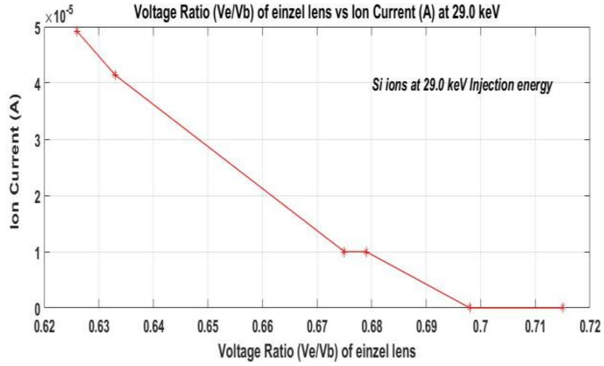

Fig. 17 Voltage ratio (Ve/Vb) vs. Ion beam current at 29.0 keV

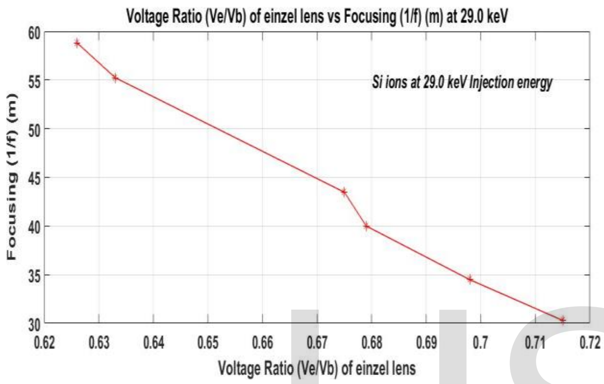

Fig. 18 Voltage ratio (Ve/Vb) vs. Focusing (1/f) at 29.0 keV

For beam acceleration, einzel lens settings also varies with terminal voltage. In the next experiment, einzel lens and the accelerator tank voltage are varied and by hit and trial and we find the maximum current at first faraday cup on the post-acceleration beamline (FC02-1). Here we used SNICS II source for the production of silver (Ag) ions. The data obtained from the AccelNET control system is given in **Table 9**. A surface plot between einzel lens voltage, tank voltage and faraday cup current (FC02-1) is generated in MATLAB, shown in **Fig. 19**.

From **Table 9** and **Fig. 19**, it is concluded that the best settings for an einzel lens voltage and tank voltage are at -4 kV and 0.3 MV respectively. The faraday cup current (FC02-1) at these settings is maximum that is 4.34×10^{-8}Amperes. This conclusion is drawn on the basis of hit and trail method that is by manually increasing or decreasing the lens voltage and accelerator tank voltage and observing the value of current at the faraday cup (FC02-1). The point at which the maximum current is achieved is the desired value of setting for einzel lens voltage and tank voltage.

Table 9 – Data from AccelNET control system

TrvVC / EL (kV)	Tank voltage (MV)			
	0.2 MV	0.3MV	0.4 MV	0.5 MV
	Faraday Cup Current FC02-1 (A)			
0	1.32×10^{-8}	4.24×10^{-8}	3.26×10^{-8}	2.01×10^{-8}
-2	1.36×10^{-8}	4.31×10^{-8}	3.15×10^{-8}	2.00×10^{-8}
-4	1.47×10^{-8}	4.34×10^{-8}	3.01×10^{-8}	1.94×10^{-8}
-6	1.74×10^{-8}	4.27×10^{-8}	2.77×10^{-8}	1.89×10^{-8}
-8	2.21×10^{-8}	4.03×10^{-8}	2.51×10^{-8}	1.78×10^{-8}
-10	2.85×10^{-8}	3.13×10^{-8}	2.14×10^{-8}	1.70×10^{-8}
-12	2.51×10^{-8}	2.16×10^{-8}	1.78×10^{-8}	1.53×10^{-8}
-14	1.35×10^{-8}	1.44×10^{-8}	1.41×10^{-8}	1.35×10^{-8}
-16	7.02×10^{-9}	9.09×10^{-9}	1.05×10^{-8}	1.16×10^{-8}
-18	3.98×10^{-8}	5.80×10^{-9}	7.68×10^{-9}	9.33×10^{-9}

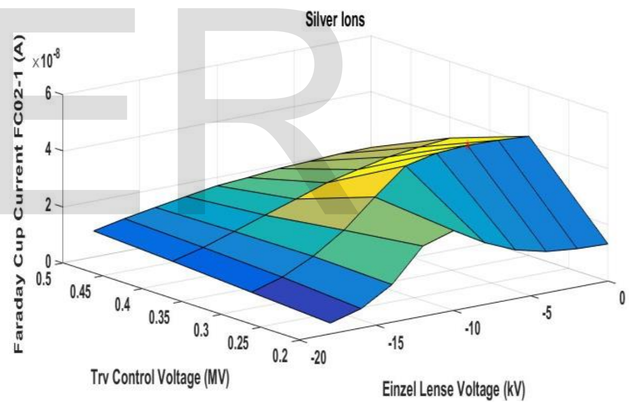

Fig. 19 Einzel lens voltage vs. Trv control voltage for silver ions

3 Results and Discussion

Beam tuning is an art, to obtain the desired beam current and beam profile at the end-stations for use in various material science experiments. Fine tuning of voltages and currents of accelerator beam-handling components will result in maximum beam current. Since the effect of different voltages and currents is inter-linked, optimum results are sometimes not achieved. To gain optimum results at pre-acceleration beamline, we performed several experiments at accelerator lab (CASP). The results of these experiments for switching magnets, electrostatic X-Y steerers and electrostatic lens (einzel lens) have already been presented. Higher injection energy is necessary to reduce the loss of beam in accelerators; as the negative ions generated by ion sources have loosely bounded electrons in their outer shells and are likely to lose electrons during interactions with the residual gas molecules present in the injection system, it is essential that they spend minimum time in the beam line before reaching the low energy accelerating tube. Magnet current settings are derived for different atomic weights and injection energies. The formula of switching magnet current calculates optimized value of current. As the atomic weight and initial energy provided by the ion source increases, the magnet current increases. The magnet current controls the bending of ions; for a particular mass and energy, greater the magnet current, the lesser the beam is deflecting. Hence the x-steerer voltage required after the selection of a particular singly charged ion by magnet is less, since the beam is already aligned in horizontal direction through the switching magnet. Steering in the vertical direction is required where the beamlines are not properly aligned. The adjustments of steering device must be done carefully, too much adjustment will result in the loss of beam. Summary of optimized settings for switching magnet current is given in **Table 10**.

Table 10 – Optimized magnet current for different ion species

Particle	Charged state	Injected Energy (keV)	I observed (A)	I calculated (A)
^{1}H	1	30.7	3.4	3.798
^{4}He	1	37.3	7.5	8.333
^{28}Si	1	28.7	16.9	19.37
^{63}Cu	1	30.0	26.22	29.78
^{197}Au	1	31.0	47.1	53.31

Einzel lens settings depends on the voltage ratio (R); the ratio between the einzel lens voltage and injector potential. Best focusing is obtained for R in the range of $0 < R < 1$. Greater the R differs from unity, the stronger is the focus provided by lens. Also the beam current at FC 02-1 is analyzed at different lens voltage and terminal voltages of tank for Ag ions. Beam current at FC 02-1 depends not only on the einzel lens voltage settings but also depends on accelerator tank voltage and stripping gas pressure for nitrogen.

4 Conclusions

Following conclusions may be drawn from the research reported in this paper.

1. Tuning of accelerator and its components involves different voltages and currents that are inter-linked.
2. The formulas discussed for low energy beamline components make it easier to find the optimized settings of these components.
3. Higher injection energy is desirable to reduce the beam losses.
4. The formula of Switching magnet current approximately calculates the optimized value of current.
5. The effect of X-steerer voltage and magnet current is inter-linked.
6. Steering in the vertical direction is required where the beamlines are not properly aligned.
7. Einzel lens settings depends on the voltage ratio (R); the ratio between the einzel lens voltage and injector potential.

5 Acknowledgments

The author wish to acknowledge the support provided for this research to the supervisor Dr. Engr. S.M. Haider Aejaz for his patient guidance, enthusiastic encouragement, immense knowledge and useful critiques of this research work and development. The author is also thankful to the Chairperson Dr. Engr. Junaid Zafar and all other faculty members of Electrical Engineering Department, GC University Lahore. Finally, the author is thankful to the parents for their efforts and for providing all the necessity and their well wishes.

6 References

[1] G. Amsel, M. Menu, J. Moulin, and J. Salomon, "The 2 MV Tandem Pelletron Accelerator of the Louvre Museum", *Nuclear Instruments and Methods in Physics Research* B45, Jan., pp.296- 301, 1990.

[2] Helmut Wiedemann, *Particle Accelerator Physics*. Cham, Switzerland: Springer, 2015.

[3] Sabah N. Mazhir, "Generated and shifted of Ion beams By Electrostatic Lenses (Einzel lens)," *Baghdad Science Journal*, vol. 12, no.4, Jan., pp. 814-820, 2015.

[4] Orhan T. Celiker, "Optimization of electron optics in a resonator cavity using Nelder-Mead simplex search for the quantum electron microscope," M.S. thesis, Massachusetts Institute of Technology, Massachusetts, 2015.